Recent Increases in Water Column Denitrification in the Seasonally Suboxic Bottom Waters of the Santa Barbara Basin

Margot E. White[1] [iD], **Patrick A. Rafter[2]** [iD], **Brandon M. Stephens[3]** [iD], **Scott D. Wankel[4]**, and **Lihini I. Aluwihare[1]**

[1]Scripps Institution of Oceanography, University of California, San Diego, San Diego, CA, USA, [2]Department of Earth System Science, University of California, Irvine, Irvine, CA, USA, [3]Marine Science Institute and Department of Ecology, Evolution, and Marine Biology, University of California, Santa Barbara, Santa Barbara, CA, USA, [4]Woods Hole Oceanographic Institution, Woods Hole, MA, USA

Abstract Denitrification in the anoxic sediments of the Santa Barbara Basin has been well documented in the historic and modern record, but the regulation of and frequency with which denitrification occurs in the overlying water column are less understood. Since 2004, the magnitude and speciation of redox active nitrogen species in bottom waters have changed markedly. Most notable are periods of decreased nitrate and increased nitrite concentrations. Here we examine these changes in nitrogen cycling as recorded by the stable isotopes of dissolved nitrate from 2010–2016. When compared to previous studies, our data identify an increase in water column denitrification in the bottom waters of the basin. Observations from inside the basin as well as data from the wider California Current Ecosystem implicate a long-term trend of decreasing oxygen concentrations as the driver for these observed changes, with ramifications for local benthic communities and regional nitrogen loss.

Plain Language Summary The current chemical environment of the deep Santa Barbara Basin is unprecedented in the 30 years since measurements began, suggesting that a regional change in ocean chemistry has occurred over this time period. Here we use stable isotope measurements of nitrate to examine how the nitrogen cycle in the deep part of the basin has changed, documenting a recent increase in the amount of nitrate being removed from the water column at this location. Nitrogen removal in the dark ocean, known as denitrification, occurs when microbes utilize nitrate for respiration in the absence of oxygen. Such a process is consistent with the extremely low or absent oxygen concentrations that accompany the altered nitrate isotope signatures we measured in this study. Denitrification in sediments is common in the Santa Barbara Basin, but extensive water column denitrification has not been previously documented. Loss of nitrate from the water column can have important consequences for the balance of nutrients that support primary production in the ocean. These changes appear to be an effect of decreasing oxygen concentrations observed on a regional scale in the North Pacific Ocean, a trend which is likely to continue as the oceans warm.

1. Introduction

The Santa Barbara Basin (SBB) is located southeast of Point Conception, where strong upwelling of nutrients fuels primary productivity in local surface waters. Bound by the Channel Islands to the south and shallow sills to the east and west, the bottom waters of the basin are isolated from intensive circulation. This reduced ventilation combined with the remineralization of organic matter results in the rapid removal of oxygen from water depths below the 475 m sill (Goericke et al., 2015). During the winter or spring, when upwelling is strongest, denser oxygen-rich waters are brought up over the sill, temporarily reoxygenating bottom waters (Reimers et al., 1990; Roach et al., 2013; Figure 1). However, reoxygenation is often short-lived—within a few months oxygen has again been completely utilized, returning the basin to a suboxic state (Goericke et al., 2015; Reimers et al., 1990). Drawdown of oxygen within the basin plays an important role in regulating the redox regime and, by extension, the geochemical cycling of elements in both sediments and the water column. The 30-year, quarterly time series of the SBB provided by the California Cooperative Fisheries Investigation (CalCOFI) program has delivered important insights into the dynamics of the basin environment (Goericke et al., 2015; Reimers et al., 1990). One prominent feature in the CalCOFI
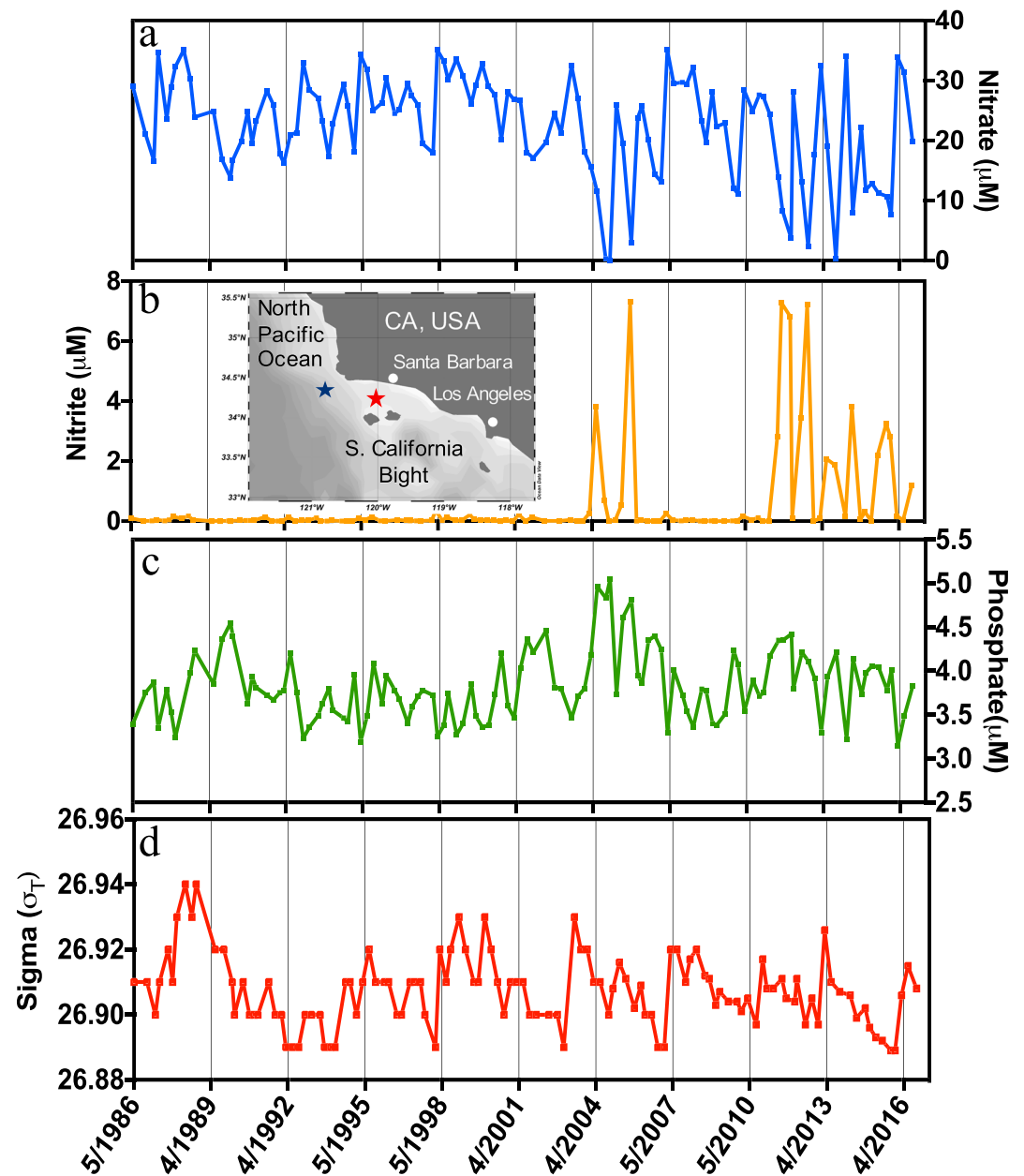
Figure 1. Time series of CalCOFI data at 570 m in the Santa Barbara Basin. The inset map shows the location of the Santa Barbara Basin in red and CalCOFI station 80.55 in blue. Starting in 2004 there are time periods where nitrate (a) is close to zero, corresponding with periodic large increases in nitrite (b). Phosphate concentrations (c) are broadly representative of time since last flushing, where phosphate accumulates between flushing events. Density (d) also provides a history of flushing events, where increases in density identify periods of flushing.

time series is the removal of nitrate (NO_3^-) from bottom waters due to denitrification (Goericke et al., 2015) —where NO_3^- is used as the terminal electron acceptor of the microbial electron transport chain, typically in support of heterotrophic remineralization of organic carbon (Körner & Zumft, 1989). By converting bioavailable NO_3^- to nitrogen gas, denitrification represents an important sink in the global nitrogen cycle (Brandes & Devol, 2002; Gruber & Sarmiento, 1997).

Previous studies of the SBB document significant changes in biogeochemistry since the time series began in the 1980s (Bograd et al., 2008; Goericke et al., 2015; Wang et al., 2017). The most pronounced of these changes has been in bottom water nitrite (NO_2^-) concentrations, which in recent years have increased by over an order of magnitude (Goericke et al., 2015; Figure 1b). In general, accumulation of nitrite to this

degree in the ocean is rare—occurring most commonly in water column oxygen-deficient zones (Buchwald & Casciotti, 2013; Casciotti, 2016a; Casciotti et al., 2013; Gaye et al., 2013; Peters et al., 2016). Nitrite is an intermediate in both the nitrification and denitrification pathways, and under low-oxygen conditions, one or both processes may contribute to its accumulation (Goericke et al., 2015; Peng et al., 2016).

Denitrification can occur in both sediments and the water column and observed changes in water column NO_3^- and NO_2^- concentration do not necessarily reflect the location of denitrification. However, well-established differences in the extent of nitrate isotope fractionation during water column denitrification relative to sediment-hosted denitrification have proven useful for apportioning their relative roles in the NO_3^- budget of the SBB and elsewhere (e.g., Sigman et al., 2003). Biological transformations often impart strong isotopic fractionation, where the more rapid reaction of lighter isotopes enriches heavier isotopes (^{15}N or ^{18}O) in the reactant pool relative to their starting distribution. The relative strength of this isotopic discrimination is represented by the isotope effect or fractionation factor and is expressed (in units of per mil, ‰) as ε (where $\varepsilon = [1 - (k^{heavy}/k^{light})] \times 1,000$, and k represents the reaction rate constant of the light or heavy isotope as denoted). The isotope effect associated with water column denitrification (ε_{wc}), is usually estimated to be between 20‰ and 30‰ (Barford et al., 1999; Brandes et al., 1998; Lehmann et al., 2003; Marconi et al., 2017), though recent work suggests that values may be lower (~15‰) under conditions typical of the open ocean (Kritee et al., 2012; Marconi et al., 2017; Sigman et al., 2009). In contrast, sedimentary denitrification (ε_{sed}) has been found to exhibit very small net fractionation, where complete utilization results in little to no NO_3^- returning to the water column after entering the sediments (Brandes & Devol, 1997). This anticipated difference between ε_{wc} and ε_{sed} was used as a framework to interpret $\delta^{15}N_{NO3}$ and $\delta^{18}O_{NO3}$ measurements from the SBB between 1995 and 1999 and indicated a dominant contribution from sedimentary denitrification (Sigman et al., 2003). That study found that water column denitrification in the SBB accounted for less than 15% of total N loss. During the same time period, CalCOFI observed no NO_2^- accumulation and bottom water NO_3^- concentrations remained above 12 μM.

In order to more definitively determine whether an increase in water column denitrification was underlying recent changes in SBB nitrogen cycling, we measured $\delta^{15}N_{NO3}$ and $\delta^{18}O_{NO3}$ in seawater samples taken during CalCOFI cruises from 2010–2016. In the SBB, where restricted circulation exacerbates biogeochemical changes occurring elsewhere in the region, an altered N Cycle may be the "canary in the coal mine" for long-term trends of warming and deoxygenation in the source waters of the productive California Current Ecosystem.

2. Materials and Methods

Samples were collected during CalCOFI cruises from 2010-2016 at station 081.8 046.9 in the center of the SBB (approximately 34.28°N and 120.02°W). Typically, three depths below the 475m sill were included—nominally 515, 540, and 570 m. Samples for nitrate and nitrite isotopes were filtered through GF/F filters (0.7 μm pore size) directly from Niskin bottles mounted on a standard conductivity-temperature-depth rosette system, and frozen until analysis. Ancillary physical and chemical data (Figure 1) were collected and analyzed by the CalCOFI program as described at http://calcofi.org. Nutrient concentrations were measured immediately or else refrigerated and measured within 16 hr. Accuracy and precision for NO_3^- and NO_2^- concentration are 0.05 and 0.01 μM, respectively. The detection limit is 0.02 μM for nitrate plus nitrite. Estimated precision for oxygen concentration measurements is 0.9 μM, though in the presence of nitrite greater than 1 μM, oxygen measurements can be erroneously high (Bograd et al., 2008). For this reason, oxygen measurements from below the sill are not discussed here as they lack the necessary precision.

Nitrogen and oxygen isotopes of NO_3^- were analyzed using the denitrifier method (Casciotti et al., 2002; Sigman et al., 2001). Samples from 2010–2012 were measured according to Rafter & Sigman, 2016. Those from 2013–2015 were measured according to Buchwald et al., 2018. Briefly, sample N_2O was purified using a customized purge and trap system and analyzed on a continuous flow IsoPrime 100 isotope ratio mass spectrometer. NO_2^- concentrations greater than 2% of $NO_3^- + NO_2^-$ were removed by addition of sulfamic acid prior to injection (Granger & Sigman, 2009). Corrections for drift, size, and fractionation of O isotopes during bacterial conversion were carried out using NO_3^- reference materials USGS 32, USGS 34, and USGS

35 (McIlvin & Casciotti, 2011). Typical reproducibility for $\delta^{15}N_{NO3}$ and $\delta^{18}O_{NO3}$ measurements was $\pm0.2‰$ and $0.4‰$, respectively. Samples with less than 1-μM N were not analyzed.

Nitrogen isotopes of NO_2^- were analyzed using the sodium azide method, in which NO_2^- is quantitatively converted to N_2O by addition of an acetic acid buffered sodium azide solution (McIlvin & Altabet, 2005). Reported $\delta^{15}N_{NO2}$ values were normalized against internal nitrite isotope reference standards WILIS 10 ($-1.7‰$) and WILIS 11 ($+57.1‰$) (Wankel et al., 2017). Typical reproducibility for $\delta^{15}N_{NO2}$ is $\pm0.1‰$.

3. Results

Measured NO_3^- isotope values increased as NO_3^- concentrations were drawn down, from values as low as $+9.9‰$ up to $+44.3‰$ for $\delta^{15}N_{NO3}$ and $+6.6‰$ up to $+29.3‰$ for $\delta^{18}O_{NO3}$ (Figures 2c and 3a). We also calculated $\Delta(15,18)$, where $\Delta(15,18) = (\delta^{15}N - \delta^{15}N_{source}) - (\delta^{18}O - \delta^{18}O_{source})$. The source isotopic signature of NO_3^- was assigned as $+8.5‰$ for $\delta^{15}N$ and $+4.6‰$ for $\delta^{18}O$ based on the average signature between 300 and 500 m outside the basin (Figure 1). Values of $\Delta(15,18)$ varied between $-1.6‰$ and $+11.9‰$ (Figure 2).

Example water column NO_3^- profiles from 2011–2012 identify the progression of denitrification as the basin becomes isolated between flushing events (Figure 3a). At depths below 500 m, NO_3^- isotope values increase as NO_3^- concentration decreases from Spring 2011 to Fall 2012. Flushing in Spring 2012 with waters rich in NO_3^- then resets concentrations and isotope signatures by diluting the denitrification signal. As evidenced from time series (Figure 2) and depth profiles (Figure 3a) NO_3^- isotope values changed in parallel across several depths, and the most enriched values at each depth accompanied maximum NO_2^- and minimum NO_3^- concentrations. For the five samples where both were measured, $\delta^{15}N_{NO2}$ was between 24.4‰ and 33.3‰ lighter than the companion $\delta^{15}N_{NO3}$ and largely changed in parallel with $\delta^{15}N_{NO3}$ (Table S1 in the supporting information).

To identify mechanisms responsible for N removal in the basin, we calculated apparent isotope fractionation factors (e.g. $^{15}\varepsilon_{app}$) from NO_3^- isotope data using a closed system, Rayleigh fractionation model, where

$$\delta^{15}N = \delta^{15}N_{source} - {}^{15}\varepsilon_{app} \times \ln\left([NO_3^-]/[NO_3^-]_{initial}\right)$$

Assuming a unidirectional transformation occurring in a closed system, a single, linear relationship would be expected in a plot of $\ln[NO_3^-]$ versus $\delta^{15}N_{NO3}$ or $\delta^{18}O_{NO3}$. Across our data set several different slopes were observed (Figures 3b and 3c), which indicated that ε_{app} varied. To examine the range, we focused on $^{15}\varepsilon_{app}$ and calculated a value for each NO_3^- isotope data point according to the rearranged equation:

$$^{15}\varepsilon_{app} = -\left(\delta^{15}N - \delta^{15}N_{source}\right)/\ln\left([NO_3^-]/[NO_3^-]_{initial}\right)$$

The $[NO_3^-]_{initial}$ was calculated from N* (Gruber & Sarmiento, 1997) according to $[NO_3^-]_{initial} = [PO_4^{3-}] \times \frac{N}{P}$; where N:P was 12.6:1 based on the $NO_3^-:PO_4^{3-}$ ratio outside the basin (CalCOFI station 80.55) at depths between 300 and 500 m. Initial $\delta^{15}N_{NO3}$ corresponded to the source values discussed previously, $+8.5‰$ for $\delta^{15}N$ and $+4.6‰$ for $\delta^{18}O$. Fractionation factors ranged from 2.7‰ to 13.3‰ for $^{15}\varepsilon_{app}$.

The variability in these ε_{app} values, which integrate all N loss processes over the time since the last flushing, likely resulted from differing contributions of sedimentary and water column denitrification to N removal from SBB bottom waters. If we assume that sedimentary denitrification consumes NO_3^- with an $^{15}\varepsilon$ of 1.5‰, while water column denitrification exhibits an $^{15}\varepsilon$ of 25‰, then the relative contribution of water column and sedimentary denitrification to each calculated ε_{app} value can be estimated from a two end-member isotope mixing model, assuming no other processes altered NO_3^- (Peters et al., 2018; Sigman et al., 2003; SI). This calculation suggested that the percent of nitrate loss occurring in the water column ranged from 0% up to 50% from 2010–2016.

We additionally estimated ε_{app} by isolating consecutive cruises where the concentration and isotopic signature of NO_3^- appeared to be unaffected by flushing (e.g., Figure 3a). During such time periods, NO_3^- continuously decreased from one cruise to the next, presumably due to denitrification, while its isotopic signature increased (Table S2). We isolated 12 such periods in the time series and calculated 12 $^{15}\varepsilon_{app}$
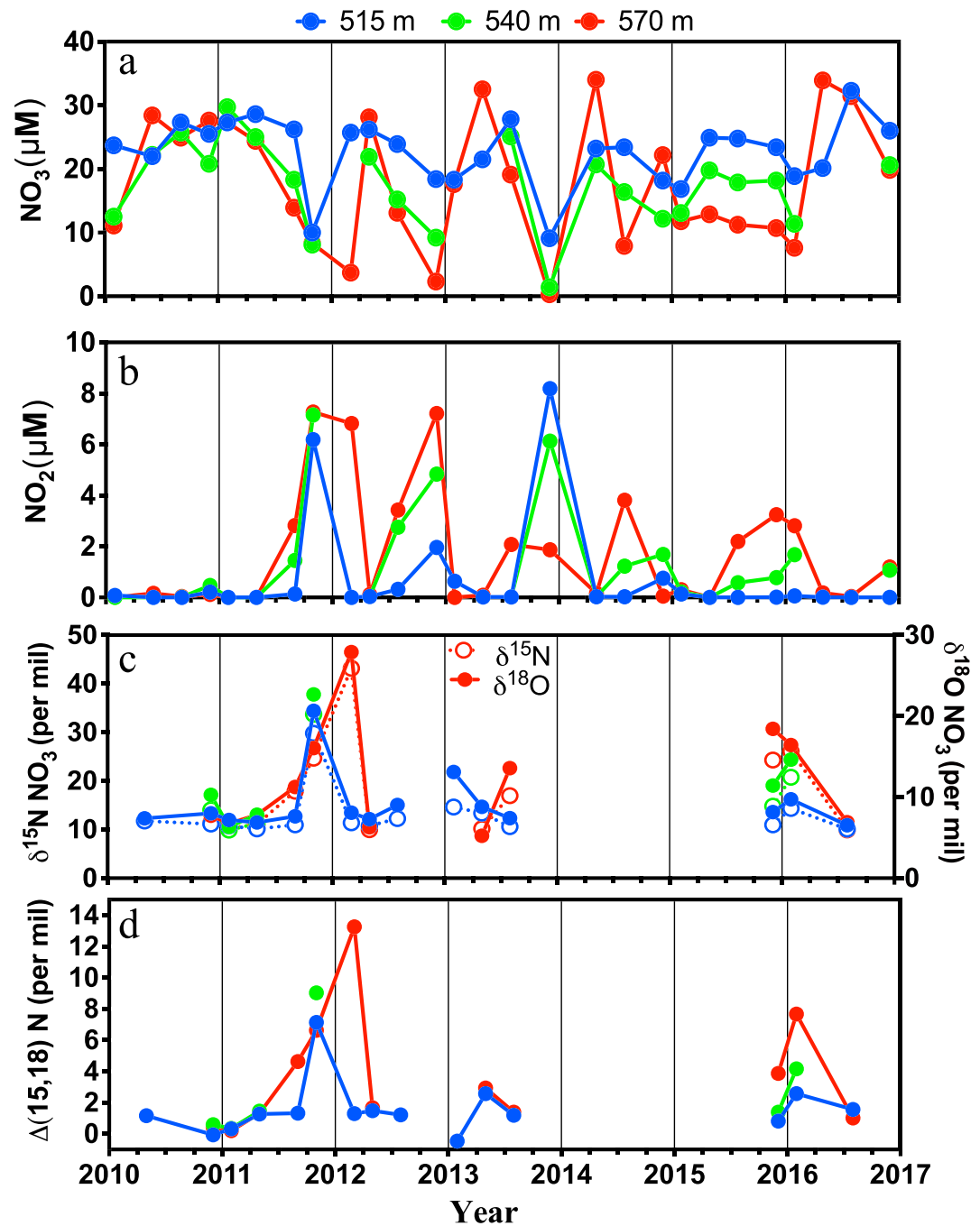
Figure 2. Nitrate and nitrite concentrations and nitrate isotope measurements from three depths. Time periods of low nitrate (a) and high nitrite (b) correspond to increased enrichment in isotope values (c) as well as greater deviation between nitrogen and oxygen isotopes of nitrate (d).

values. These values ranged from 8.1‰ to 24.3‰ (Table S2). Applying the same isotopic mass balance for ε as above, we found that **in situ** nitrogen loss in the water column ranged from 28% to 97% of the total, for these time periods.

Values of $\Delta(15,18)$ are expected to be close to 0‰ if denitrification is the primary process altering NO_3^- concentrations and isotopes. However, this value increased together with $\delta^{15}N_{NO3}$ and $\delta^{18}O_{NO3}$ (Figure 2d) suggesting that NO_2^- reoxidation could influence NO_3^- isotopes. To test this hypothesis, we adopted a previously described dual nitrate isotope model framework (Granger & Wankel, 2016), which explicitly
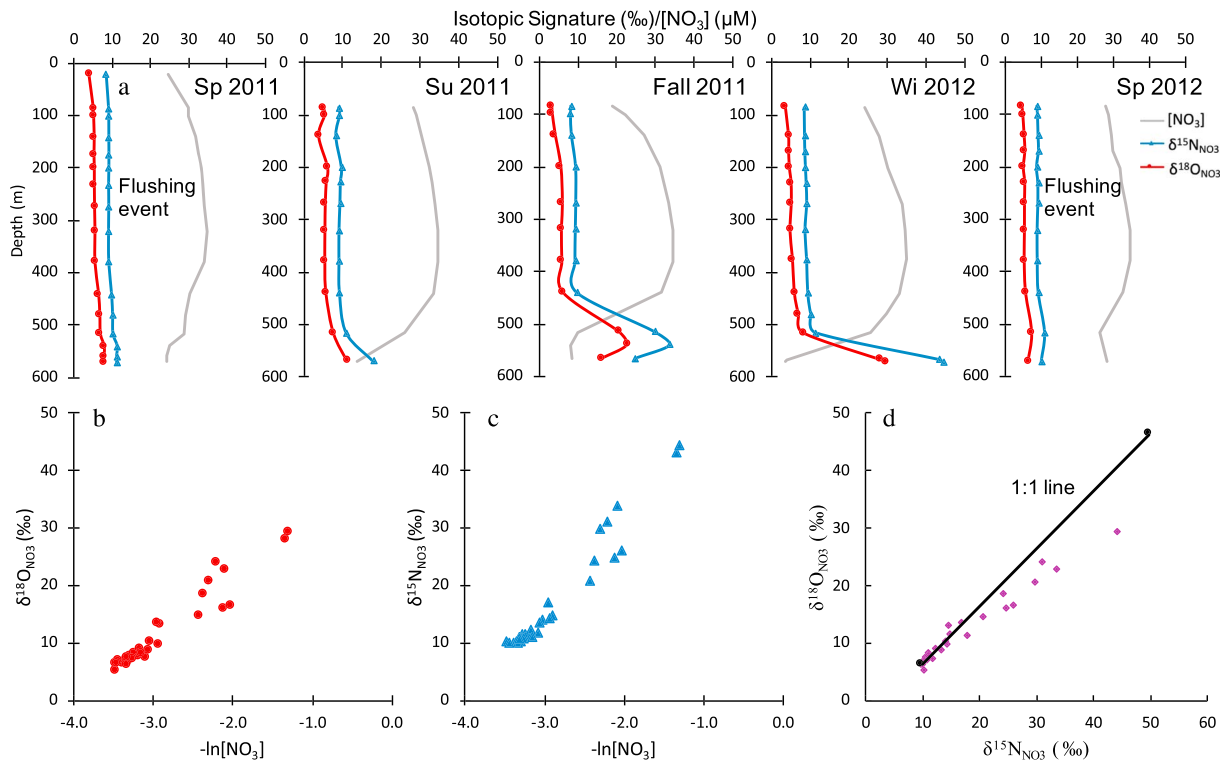
Figure 3. Profiles from five cruises are shown in (3a) beginning with a flushing event in the spring of 2011. Following the flushing, the basin becomes deoxygenated and nitrogen is removed as isotopes become progressively more enriched until another flushing event in the following spring. Figure 3b shows $\delta^{18}O_{NO3}$ for all samples below the sill depth versus the negative natural log of nitrate concentration. Unidirectional consumption of nitrate in a closed system yields a straight line with the slope reflecting the apparent $^{18}\varepsilon$. Figure 3c shows the same, but for $\delta^{15}N_{NO3}$. Figure 3d plots $\delta^{18}O_{NO3}$ versus $\delta^{15}N_{NO3}$ with the black line showing a 1:1 relationship between the two.

includes nitrate reduction (**NAR**), nitrite reduction (**NIR**) and nitrite reoxidation to nitrate (**NXR**), to identify processes influencing the isotopic signature of the standing NO_3^- pool. Pooling data from all sampling time points, the model iterates to minimize differences from observed NO_3^- concentrations and isotopic signatures by optimizing $^{15}\varepsilon$ values for NO_3^- reduction ($^{15}\varepsilon_{NAR}$; assuming the $^{15}\varepsilon_{NAR} = ^{18}\varepsilon_{NAR}$; Granger et al., 2008), NO_2^- reduction ($^{15}\varepsilon_{NIR}$) and NO_2^- reoxidation ($^{15}\varepsilon_{NXR}$), as well as the relative flux of NO_2^- reoxidation to NO_3^- reduction (NXR/NAR), in a series of governing isotope mass balance equations (Granger & Wankel, 2016). Values for the inverse kinetic oxygen isotope effect of NO_2^- oxidation ($^{18}\varepsilon_{NXR}$) and the normal kinetic isotope effect for incorporation of O from water during NO_2^- oxidation ($^{18}\varepsilon_{k,H2O}$) were assumed to be $-4‰$ and $+14‰$, respectively (Buchwald & Casciotti, 2010) and the $\delta^{18}O_{NO2}$ was assumed to reflect a 13.5‰ higher equilibrium isotope composition (Casciotti et al., 2007) with respect to seawater ($\delta^{18}O_{SW} = 0‰$). Results of optimized model fits yielded values of $8.8 \pm 0.7‰$ for $^{15}\varepsilon_{NAR}$, $9.7 \pm 4.9‰$ for $^{15}\varepsilon_{NIR}$, $-32.9 \pm 16.8‰$ for $^{15}\varepsilon_{NXR}$ and 0.10 ± 0.05 for NXR/NAR. If $^{15}\varepsilon_{NAR}$, the fractionation factor for the integrated (i.e., water column and sedimentary) process of NO_3^- reduction reflected in the pooled NO_3^- samples, is treated like $^{15}\varepsilon_{app}$, then revisiting the mass balance calculation from above suggests an average of $37 \pm 3\%$ of nitrate loss attributable to water column denitrification during our study period.

4. Discussion

Patterns of increased nitrogen loss and elevated NO_2^- in SBB bottom waters are consistent with regional (and global) progression toward expanding oxygen depletion in nearshore environments. Below we discuss our isotope data and argue that water column denitrification has greatly increased in the years since 2004, resulting in periodic accumulation of NO_2^- to levels unprecedented in the context of the CalCOFI record

and a pronounced enrichment in $\delta^{15}N_{NO3}$ and $\delta^{18}O_{NO3}$. Furthermore, we posit that these trends are the result of decreased oxygen delivery to the basin.

4.1. Evidence of Water Column Denitrification

The accumulation of NO_2^- in the SBB (up to 8.19 μM, Figures 1 and 2) contrasts markedly with previous basin records (since 1986; Goericke et al., 2015) and is consistent with, or at times greater than, observations from open ocean oxygen deficient zones (Casciotti, 2016a; Gaye et al., 2013; Martin & Casciotti, 2017). Similarly, periods of low NO_3^- have increased in frequency in recent years (Figure 1; Goericke et al., 2015). The combined time series clearly shows that periods of low NO_3^- correspond temporally with elevated NO_2^- (Figure 1) and greater enrichment in $\delta^{15}N_{NO3}$ and $\delta^{18}O_{NO3}$ (Figure 2). These records are all consistent with greater incidence of water column denitrification since ~2004.

We calculated the relative importance of water column denitrification using three different approaches. First, we used ε_{app} values calculated using a closed system, Rayleigh model to estimate percent water column denitrification since last flushing. We found that up to 50% of N removal was mediated by water column denitrification. However, one limitation of this calculation is the use of PO_4^{3-} concentrations in the basin to estimate initial NO_3^-. In low-oxygen environments, respiration is not the only source of PO_4^{3-} as PO_4^{3-} bound to iron particles can be released from reducing sediments into the water column (Bourbonnais et al., 2013; King & Barbeau, 2011; Peters et al., 2018; Reimers et al., 1990). Thus, it is possible that the N:P approach taken here overestimated $[NO_3^-]_{initial}$ at times, as has been concluded elsewhere (Hu et al., 2016; Peters et al., 2018). For this reason, we also estimated ε_{app} using the change in isotopic composition internal to the basin between two time points where NO_3^- continued to decrease. With this approach, the initial NO_3^- concentration is that measured at the first time point. Using this method, we found that on occasion, up to 97% of NO_3^- loss in the basin resulted from water column denitrification (Table S2). Time periods with such high N loss from water column denitrification are typically accompanied by very low NO_3^-. For example, for this time period, the NO_3^- at 570 m was 3.7 μM and sedimentary denitrification would have been limited due to low diffusion from the water column. The two estimates are distinct because the former examines the time period since the basin was flushed, whereas the latter captures the shorter time period between two cruises. Furthermore, a model that examined the influence of processes other than denitrification on NO_3^- isotopes estimated that an average of 37 ± 3% of nitrate loss could be attributed to water column denitrification during our study period. Despite the different assumptions, processes, and time periods captured in each method, they all identify the importance of water column denitrification and exceed the previous estimate of around 15% reported in Sigman et al., 2003.

Many processes can act to dilute the observed ε_{app}, including partial flushing and nitrite reoxidation (see below). However, increasing ε_{app} with decreasing NO_3^- can only be explained by greater influence of water column denitrification. Thus, our data require extensive water column denitrification, in addition to sedimentary denitrification, to be taking place in the basin when NO_3^- is drawn down to its lowest levels. Nitrogen isotopes of NO_2^- were significantly depleted compared to $\delta^{15}N_{NO3}$ (by 24.4‰ to 33.3‰), and they increased in tandem, indicating that NO_3^- reduction is the most likely source of NO_2^- in the system (Table S1).

4.2. Evidence of Nitrite Reoxidation

If denitrification is the only process affecting NO_3^- then equal increases in both $\delta^{15}N$ and $\delta^{18}O$ are expected (Granger et al., 2008). While earlier observations noted a consistent 1:1 relationship between $\delta^{15}N_{NO3}$ and $\delta^{18}O_{NO3}$ in the SBB, these were restricted to conditions of limited NO_3^- consumption (Sigman et al., 2003). Here, we observe higher relative increases in $\delta^{15}N$ values compared to corresponding $\delta^{18}O$ values when NO_3^- loss was greater, as is visible in Δ(15,18) values exceeding 0‰ (Figures 2d) and a slope <1 in a plot of $\delta^{15}N_{NO3}$ versus $\delta^{18}O_{NO3}$ (Figure 3d). The departure from the expected relationship between $\delta^{15}N_{NO3}$ and $\delta^{18}O_{NO3}$ is most prominent during periods of NO_2^- accumulation in the water column. Such deviations are commonly observed in oxygen-deficient zones and have generally been interpreted as evidence for the influence of NO_2^- reoxidation to NO_3^- (Casciotti, 2016a; Granger & Wankel, 2016; Sigman et al., 2005).

The observed deviation from 1:1 can be linked to several interrelated mechanisms (Casciotti, 2016b; Granger & Wankel, 2016). Foremost, if NO_2^- becomes reoxidized to NO_3^-, one of the required oxygen atoms derives from the surrounding water, contributing to a difference between $\delta^{15}N_{NO3}$ and $\delta^{18}O_{NO3}$ (Buchwald & Casciotti, 2010). Indeed, our data reflect lower than expected $\delta^{18}O_{NO3}$ relative to observed $\delta^{15}N_{NO3}$, as might be predicted as a progressive consequence of the incorporation of low $\delta^{18}O$ from seawater (~0‰;Buchwald & Casciotti, 2010 ; Casciotti, 2016a). Previous work has described a phenomenon similar to that observed here, under conditions where NO_3^- consumption is extensive and $\delta^{15}N_{NO3}$ is significantly elevated (Casciotti et al., 2013; Granger & Wankel, 2016). As presented in Granger and Wankel (2016), the disparity from 1:1 is also partially explained by the inverse isotope effect imparted on NO_2^- during oxidation to NO_3^-, in which heavier isotopes preferentially accumulate in the product NO_3^- pool and the effect on N isotopes is greater than on O isotopes (Buchwald & Casciotti, 2010; Casciotti, 2016a). Overall, existing studies confirm that $\delta^{15}N_{NO3}$ should become more enriched than $\delta^{18}O_{NO3}$ during nitrite reoxidation. Thus, it seems likely that NO_2^- re-oxidation is contributing to the measured isotopic composition of NO_3^-. This effect becomes more prominent at higher degrees of NO_3^- consumption, NO_2^- accumulation and associated extremes in isotopic composition. Indeed, model fits to the dual isotope trajectories presented here suggest that as much as 10% of the standing NO_3^- pool may derive from a reoxidative NO_2^- flux.

Notably, the model results fail to adequately reproduce the observed low $\delta^{15}N_{NO2}$ values (Table S1). One possible explanation for this may be the presence of a source of NO_2^- not linked to nitrate reduction, such as ammonia oxidation, although accumulation of ammonium is rarely observed in the basin. Overall, the important consequence of any nitrite reoxidation is that accurate estimates of the exact extent of water column denitrification cannot be made with these isotope data alone. Furthermore, the added perspective of $\delta^{18}O_{NO3}$ drew attention to the fact that $\delta^{15}N_{NO3}$ in the bottom waters of the SBB likely does not reflect the singular process of NO_3^- reduction, but rather the confluence of an active redox cycling between NO_3^- and NO_2^-.

4.3. External Influences on Bottom Water Biogeochemistry

Our data unequivocally support the importance of water column denitrification as the cause of the observed NO_2^- accumulation and NO_3^- deficit. We conclude that water column denitrification rates remained fairly low during the time period from 1986 to 2004 when NO_2^- accumulation was not observed. This is supported by the relatively higher NO_3^- concentrations during that time (Figure 1a). Goericke et al. (2015) also noted that NO_3^- removal rates appeared to increase when NO_3^- was below 15 μM, an observation that is consistent with water column denitrification rates being generally faster than sedimentary rates (Groffman et al., 2006). Those authors hypothesized that a decrease in either the frequency of flushing events or in the strength of that flushing was altering N cycling in the basin. Based on observed time series of bottom water properties, flushing events in the SBB appear to have occurred at a similar frequency over the course of the time series (Figure 1d). Furthermore, lowest NO_3^- concentrations are not consistently accompanied by the highest PO_4^{3-} concentrations, where PO_4^{3-} accumulation in bottom waters is considered to be a proxy for time since flushing (Figure 1; Goericke et al., 2015). Thus, the observed anomalous NO_2^- accumulation does not appear to be definitively related to the frequency of flushing events.

As proposed in Goericke et al. (2015), it seems that observed changes in N cycling stem from a reduction in the extent of reoxygenation during more recent flushing events, as demonstrated by decreasing oxygen concentrations at shallower basin depths (Wang et al., 2017; Figure S1). There is strong evidence that the overall internal oxygen content of the basin has decreased over the last two decades (Wang et al., 2017), which is likely related to decreasing oxygen concentrations in the CCE as a whole (Bograd et al., 2008) and the meso-pelagic North Pacific more generally (Ito et al., 2017). A shoaling of the hypoxic boundary has been observed outside the basin, suggesting that each flushing event would introduce less oxygen. It has also been noted that decreases in oxygen outside the basin appeared to be more pronounced during January to March (Bograd et al., 2008), which is the time period immediately preceding the detection of spring flushing events in the CalCOFI time series. Thus, the seasonality of deep water deoxygenation may have an outsized effect on the basin. A recent analysis of oxygen trends in the global ocean concluded that oxygen has decreased in the ocean's interior due to greater apparent oxygen utilization, which points to changes in biology or ocean physics as the primary cause of this decrease rather than decreased solubility in the surface ocean (Ito et al.,

2017). Finally, paleoceanographic evidence using Fe/Ti ratios from sediment cores collected in the basin suggest oxygen concentrations in the bottom waters over the past 15 years are the lowest observed over the last 200 years (Wang et al., 2017).

5. Conclusions

Time periods of high NO_3^- loss in the SBB appear to have increased in frequency and intensity beginning in the early 2000s, accompanied by a large periodic increase in NO_2^-. The evidence from $\delta^{15}N_{NO3}$ and $\delta^{18}O_{NO3}$ presented here shows that this increase is almost entirely due to episodic increases in water column denitrification. However, we find that the isotope values cannot be definitively used to quantify the NO_3^- loss because NO_2^- reoxidation plays a role in modifying the isotopic composition of NO_3^-. These large changes in the extent of water column denitrification appear to be linked to decreased oxygen concentrations in waters entering the basin. Thus, extreme changes in the biogeochemistry of the SBB may serve as an indicator of the state of the CCE at large, and the changes that a warming climate may bring to the region. With the shallowest sills of any of the California Borderland Basins, the current state of the SBB may foreshadow how conditions in other basins are likely to change in the future as deoxygenation and warming continue. Further work should focus on continued monitoring of this basin, perhaps including denitrification rate measurements and/or measurements of N_2/Ar. A more complete understanding of the dynamics and timing of basin flushing would also be beneficial, as well as additional modeling efforts aimed at a better constraining the effects of mixing on the complex isotope dynamics of nitrogen cycling in the anoxic bottom waters.

References

Barford, C. C., Montoya, J. P., Altabet, M. A., & Mitchell, R. (1999). Steady-state nitrogen isotope effects of N_2 and N_2O production in *Paracoccus denitrificans*. *Applied and Environmental Microbiology*, *65*(3), 989–994. Retrieved from http://www.ncbi.nlm.nih.gov/pubmed/10049852

Bograd, S. J., Castro, C. G., Di Lorenzo, E., Palacios, D. M., Bailey, H., Gilly, W., & Chavez, F. P. (2008). Oxygen declines and the shoaling of the hypoxic boundary in the California Current. *Geophysical Research Letters*, *35*, L12607. https://doi.org/10.1029/2008GL034185

Bourbonnais, A., Lehmann, M. F., Hamme, R. C., Manning, C. C., & Juniper, S. K. (2013). Nitrate elimination and regeneration as evidenced by dissolved inorganic nitrogen isotopes in Saanich Inlet, a seasonally anoxic fjord. *Marine Chemistry*, *157*, 194–207. https://doi.org/10.1016/j.marchem.2013.09.006

Brandes, J. A., & Devol, A. H. (1997). Isotopic fractionation of oxygen and nitrogen in coastal marine sediments. *Geochimica et Cosmochimica Acta*, *61*(9), 1793–1801. https://doi.org/10.1016/S0016-7037(97)00041-0

Brandes, J. A., & Devol, A. H. (2002). A global marine-fixed nitrogen isotopic budget: Implications for Holocene nitrogen cycling. *Global Biogeochemical Cycles*, *16*(4), 1120. https://doi.org/10.1029/2001GB001856

Brandes, J. A., Devol, A. H., Yoshinari, T., Jayakumar, D. A., & Naqvi, S. W. A. (1998). Isotopic composition of nitrate in the central Arabian Sea and eastern tropical North Pacific: A tracer for mixing and nitrogen cycles. *Limnology and Oceanography*, *43*(7), 1680–1689. https://doi.org/10.4319/lo.1998.43.7.1680

Buchwald, C., & Casciotti, K. L. (2010). Oxygen isotopic fractionation and exchange during bacterial nitrite oxidation. *Limnology and Oceanography*, *55*(3), 1064–1074. https://doi.org/10.4319/lo.2010.55.3.1064

Buchwald, C., & Casciotti, K. L. (2013). Isotopic ratios of nitrite as tracers of the sources and age of oceanic nitrite. *Nature Geoscience*, *6*(4), 308–313. https://doi.org/10.1038/ngeo1745

Buchwald, C., Homola, K., Spivack, A. J., Estes, E. R., Murray, R. W., & Wankel, S. D. (2018). Isotopic constraints on nitrogen transformation rates in the deep sedimentary marine biosphere. *Global Biogeochemical Cycles*, *32*, 1688–1702. https://doi.org/10.1029/2018GB005948

Casciotti, K. L. (2016a). Nitrite isotopes as tracers of marine N cycle processes. *Philosophical Transactions of the Royal Society A: Mathematical, Physical and Engineering Sciences*, *374*(2081). https://doi.org/10.1098/rsta.2015.0295

Casciotti, K. L. (2016b). Nitrogen and oxygen isotopic studies of the marine nitrogen cycle. *Annual Review of Marine Science*, *8*(1), 379–407. https://doi.org/10.1146/annurev-marine-010213-135052

Casciotti, K. L., Böhlke, J. K., McIlvin, M. R., Mroczkowski, S. J., & Hannon, J. E. (2007). Oxygen Isotopes in Nitrite: Analysis, Calibration, and Equilibration. *Analytical Chemistry*, *79*(6), 2427–2436. https://doi.org/10.1021/AC061598H

Casciotti, K. L., Buchwald, C., & McIlvin, M. (2013). Implications of nitrate and nitrite isotopic measurements for the mechanisms of nitrogen cycling in the Peru oxygen deficient zone. *Deep Sea Research Part I: Oceanographic Research Papers*, *80*, 78–93. Retrieved from https://www.sciencedirect.com/science/article/pii/S0967063713001155

Casciotti, K. L., Sigman, D. M., Hastings, M. G., Böhlke, J. K., & Hilkert, A. (2002). Measurement of the oxygen isotopic composition of nitrate in seawater and freshwater using the denitrifier method. *Analytical Chemistry*, *74*(19), 4905–4912. https://doi.org/10.1021/ac020113w

Gaye, B., Nagel, B., Dähnke, K., Rixen, T., & Emeis, K.-C. (2013). Evidence of parallel denitrification and nitrite oxidation in the ODZ of the Arabian Sea from paired stable isotopes of nitrate and nitrite. *Global Biogeochemical Cycles*, *27*, 1059–1071. https://doi.org/10.1002/2011GB004115

Goericke, R., Bograd, S. J., & Grundle, D. S. (2015). Denitrification and flushing of the Santa Barbara Basin bottom waters. *Deep-Sea Research Part II: Topical Studies in Oceanography*, *112*, 53–60. https://doi.org/10.1016/j.dsr2.2014.07.012

Granger, J., & Sigman, D. M. (2009). Removal of nitrite with sulfamic acid for nitrate N and O isotope analysis with the denitrifier method. *Rapid Communications in Mass Spectrometry*, *23*(23), 3753–3762. https://doi.org/10.1002/rcm.4307

Granger, J., Sigman, D. M., Lehmann, M. F., & Tortell, P. D. (2008). Nitrogen and oxygen isotope fractionation during dissimilatory nitrate reduction by denitrifying bacteria. *Limnology and Oceanography*, *53*(6), 2533–2545. https://doi.org/10.4319/lo.2008.53.6.2533

Granger, J., & Wankel, S. D. (2016). Isotopic overprinting of nitrification on denitrification as a ubiquitous and unifying feature of environmental nitrogen cycling. *Proceedings of the National Academy of Sciences of the United States of America*, *113*(42), E6391–E6400. https://doi.org/10.1073/pnas.1601383113

Groffman, P. M., Altabet, M. A., Böhlke, J. K., Butterbach-Bahl, K., David, M. B., Firestone, M. K., et al. (2006). Methods for measuring denitrification: Diverse approaches to a difficult problem. *Ecological Applications: A Publication of the Ecological Society of America*, *16*(6), 2091–2122. Retrieved from http://www.ncbi.nlm.nih.gov/pubmed/17205891, https://doi.org/10.1890/1051-0761(2006)016[2091:MFMDDA]2.0.CO;2

Gruber, N., & Sarmiento, J. L. (1997). Global patterns of marine nitrogen fixation and denitrification. *Global Biogeochemical Cycles*, *11*(2), 235–266. https://doi.org/10.1029/97GB00077

Hu, H., Bourbonnais, A., Larkum, J., Bange, H. W., & Altabet, M. A. (2016). Nitrogen cycling in shallow low-oxygen coastal waters off Peru from nitrite and nitrate nitrogen and oxygen isotopes. *Biogeosciences*, *13*(5), 1453–1468. https://doi.org/10.5194/bg-13-1453-2016

Ito, T., Minobe, S., Long, M. C., & Deutsch, C. (2017). Upper ocean O_2 trends: 1958–2015. *Geophysical Research Letters*, *44*, 4214–4223. https://doi.org/10.1002/2017GL073613

King, A. L., & Barbeau, K. A. (2011). Dissolved iron and macronutrient distributions in the southern California Current System. *Journal of Geophysical Research*, *116*, C03018. https://doi.org/10.1029/2010JC006324

Körner, H., & Zumft, W. G. (1989). Expression of denitrification enzymes in response to the dissolved oxygen level and respiratory substrate in continuous culture of Pseudomonas stutzeri. *Applied and Environmental Microbiology*, *55*(7), 1670–1676. Retrieved from http://www.ncbi.nlm.nih.gov/pubmed/2764573

Kritee, K., Sigman, D. M., Granger, J., Ward, B. B., Jayakumar, A., & Deutsch, C. (2012). Reduced isotope fractionation by denitrification under conditions relevant to the ocean. *Geochimica et Cosmochimica Acta*, *92*, 243–259. https://doi.org/10.1016/j.gca.2012.05.020

Lehmann, M. F., Reichert, P., Bernasconi, S. M., Barbieri, A., & McKenzie, J. A. (2003). Modelling nitrogen and oxygen isotope fractionation during denitrification in a lacustrine redox-transition zone. *Geochimica et Cosmochimica Acta*, *67*(14), 2529–2542. https://doi.org/10.1016/S0016-7037(03)00085-1

Marconi, D., Kopf, S., Rafter, P. A., & Sigman, D. M. (2017). Aerobic respiration along isopycnals leads to overestimation of the isotope effect of denitrification in the ocean water column. *Geochimica et Cosmochimica Acta*, *197*, 417–432. https://doi.org/10.1016/J.GCA.2016.10.012

Martin, T. S., & Casciotti, K. L. (2017). Paired N and O isotopic analysis of nitrate and nitrite in the Arabian Sea oxygen deficient zone. *Deep Sea Research Part I: Oceanographic Research Papers*, *121*, 121–131. https://doi.org/10.1016/j.dsr.2017.01.002

McIlvin, M. R., & Altabet, M. A. (2005). Chemical conversion of nitrate and nitrite to nitrous oxide for nitrogen and oxygen isotopic analysis in freshwater and seawater. *Analytical Chemistry*, *77*(17), 5589–5595. https://doi.org/10.1021/AC050528S

McIlvin, M. R., & Casciotti, K. L. (2011). Technical updates to the bacterial method for nitrate isotopic analyses. *Analytical Chemistry*, *83*(5), 1850–1856. https://doi.org/10.1021/ac1028984

Peng, X., Fuchsman, C. A., Jayakumar, A., Warner, M. J., Devol, A. H., & Ward, B. B. (2016). Revisiting nitrification in the Eastern Tropical South Pacific: A focus on controls. *Journal of Geophysical Research: Oceans*, *121*, 1667–1684. https://doi.org/10.1002/2015JC011455

Peters, B., Horak, R., Devol, A., Fuchsman, C., Forbes, M., Mordy, C. W., & Casciotti, K. L. (2018). Estimating fixed nitrogen loss and associated isotope effects using concentration and isotope measurements of NO3-, NO2-, and N2 from the Eastern Tropical South Pacific oxygen deficient zone. *Deep Sea Research Part II: Topical Studies in Oceanography*, *156*, 121–136. https://doi.org/10.1016/J.DSR2.2018.02.011

Peters, B. D., Babbin, A. R., Lettmann, K. A., Mordy, C. W., Ulloa, O., Ward, B. B., & Casciotti, K. L. (2016). Vertical modeling of the nitrogen cycle in the eastern tropical South Pacific oxygen deficient zone using high-resolution concentration and isotope measurements. *Global Biogeochemical Cycles*, *30*, 1661–1681. https://doi.org/10.1002/2016GB005415

Rafter, P. A., & Sigman, D. M. (2016). Spatial distribution and temporal variation of nitrate nitrogen and oxygen isotopes in the upper equatorial Pacific Ocean. *Limnology and Oceanography*, *61*(1), 14–31. https://doi.org/10.1002/lno.10152

Reimers, C. E., Lange, C. B., Tabak, M., & Bernhard, J. M. (1990). Seasonal spillover and varve formation in the Santa Barbara Basin, California. *Limnology and Oceanography*, *35*(7), 1577–1585. https://doi.org/10.4319/lo.1990.35.7.1577

Roach, L. D., Charles, C. D., Field, D. B., & Guilderson, T. P. (2013). Foraminiferal radiocarbon record of northeast Pacific decadal subsurface variability. *Journal of Geophysical Research: Oceans*, *118*, 4317–4333. https://doi.org/10.1002/jgrc.20274

Sigman, D. M., Casciotti, K. L., Andreani, M., Barford, C., Galanter, M., & Böhlke, J. K. (2001). A bacterial method for the nitrogen isotopic analysis of nitrate in seawater and freshwater. *Analytical Chemistry*, *73*(17), 4145–4153. https://doi.org/10.1021/ac010088e

Sigman, D. M., Granger, J., DiFiore, P. J., Lehmann, M. M., Ho, R., Cane, G., & van Geen, A. (2005). Coupled nitrogen and oxygen isotope measurements of nitrate along the eastern North Pacific margin. *Global Biogeochemical Cycles*, *19*, GB4022. https://doi.org/10.1029/2005GB002458

Sigman, D. M., Karsh, K. L., & Casciotti, K. L. (2009). Nitrogen isotopes in the ocean. In *Encyclopedia of ocean sciences* (pp. 40–54). https://doi.org/10.1016/B978-012374473-9.00632-9

Sigman, D. M., Robinson, R., Knapp, A. N., van Geen, A., McCorkle, D. C., Brandes, J. A., & Thunell, R. C. (2003). Distinguishing between water column and sedimentary denitrification in the Santa Barbara Basin using the stable isotopes of nitrate. *Geochemistry, Geophysics, Geosystems*, *4*(5), 1040. https://doi.org/10.1029/2002GC000384

Wang, Y., Hendy, I., & Napier, T. J. (2017). Climate and anthropogenic controls of coastal deoxygenation on interannual to centennial timescales. *Geophysical Research Letters*, *44*, 11,528–11,536. https://doi.org/10.1002/2017GL075443

Wankel, S. D., Ziebis, W., Buchwald, C., Charoenpong, C., de Beer, D., Dentinger, J., et al. (2017). Evidence for fungal and chemodenitrification based N2O flux from nitrogen impacted coastal sediments. *Nature Communications*, *8*(1), 15595. https://doi.org/10.1038/ncomms15595